Academic Journal of Science and Technology
ISSN: 2771-3032 | Vol. 10, No. 1, 2024

Magnetic Design and Electromagnetic Field Simulation of Downhole Turbine Generator

Ruyi Gou, Shunjun Long, Jinfa Zhang

School of Mechanical and Electrical Engineering, Southwest Petroleum University, Chengdu 610500, China

Abstract: With the increasing difficulty of oil and gas resources exploration and the increase of drilling operations in complex geological environments, the challenges faced by oil drilling operations are also increasing. With the continuous improvement of the intelligence of MWD/LWD drilling technology and downhole instruments, the demand for electric energy is also increasing. In order to ensure the normal operation of the equipment and the accurate acquisition of data, this paper designs a new type of external rotor downhole turbine generator, and designs the structure and parameters of the turbine generator. Finally, Ansoft Maxwell software is used to simulate and analyze the electromagnetic field of the generator. The results show that the induced electromotive force and load current waveform obtained by electromagnetic field simulation analysis have good sinusoidality. At the rated speed of 2500rpm, the effective value of the output line voltage of the turbine generator is about 49.1V, the effective value of the line current is about 10.99A, and the output power is about 841.17W, which meets the design requirements. The research has certain guiding significance for practical engineering.

Keywords: Turbine generator; structural design; parameter design; electromagnetic field simulation.

1. Introduction

China 's oil resources are widely distributed and relatively abundant, but with the continuous development of large-scale mining, crude oil production has shown a downward trend in recent years. Conventional oil and gas wells have been unable to meet the demand, and the focus of mining has also shifted from land to sea, extending from shallow to deep [1-3]. Especially in special environments such as high temperature and high pressure wells, highly deviated wells, geothermal wells, ultra-deep wells and extended reach wells, conventional tools have been unable to meet mining needs. Downhole tools require more intelligence, longer working hours, and more measurement parameters [4]. With the development of MWD technology, the increase of measurement parameters, the increase of downhole equipment complexity, the increase of well depth and horizontal section length, the increase of well temperature and the extension of MWD system running time in downhole are inevitable trends [5-7]. Therefore, the capacity and reliability of MWD power system become very important, and the demand for electric energy is also increasing [8].

In the current underground environment, the power supply system mainly relies on three main ways: battery pack power supply, cable power supply and turbine generator power supply [9,10]. However, the cable is limited by length and environmental conditions, and the scope of use may be limited by some limitations, such as limited battery life, poor applicability in high temperature environments, and environmental pollution risks [11,12] The turbine generator power supply converts the kinetic energy of the fluid into rotating mechanical energy, and then converts the mechanical energy into electrical energy through the generator. The turbine generator can make up for the shortcomings of the above two power supply methods and has higher safety performance. At present, the measurement while drilling (MWD), logging while drilling (LWD) and rotary steering system at home and abroad are all powered by turbine generators, and turbine generator power supply has gradually become the future development trend.

In order to meet the power supply requirements of downhole equipment, a new type of external rotor downhole turbine generator is designed in this paper, and the structure and parameters of the turbine generator are selected and designed. Finally, Ansoft Maxwell software is used to simulate the no-load, load and loss of the generator. The correctness of the design is verified according to the simulation results.

2. New Outer Rotor Type Downhole Turbine Generator

At present, the existing product structure of downhole turbine generator mainly includes magnetic coupling type, rotating dynamic seal hard connection type and permanent magnet and turbine fixed connection type. However, the disadvantage of the magnetic coupling type is that three kinds of permanent magnets are needed, which increases the production cost, and the structure is complex, which is not suitable for small diameter wells. The disadvantage of the rotary dynamic seal hard connection type is that when the generator is working in a high temperature and high pressure environment, the rotary dynamic seal is easy to be damaged, and the liquid flows through the inside of the generator, resulting in the generator not working properly. The disadvantage of the fixed connection between the permanent magnet and the turbine is that if there are more impurities or solid particles in the liquid, it may affect the movement of the turbine and the permanent magnet and reduce the efficiency of the system.

In order to overcome some shortcomings of the above turbine generator, a new type of external rotor downhole turbine generator is designed, and its structure is shown in Fig.1. The advantages of this structure are as follows: 1. The design of the outer rotor enables the liquid to directly drive the turbine rotation, which helps to improve the efficiency of energy conversion. 2. In the downhole high temperature environment, drilling fluid flow can take away heat, which is

conducive to heat dissipation. 3. It effectively avoids the disadvantages of dynamic seal connection easy to damage and magnetic coupling connection easy to slip out of step, and improves the stability and reliability of the system. The isolation sleeve is used to effectively protect the stator coil, prevent the drilling fluid from entering the stator coil, and reduce the risk of generator damage. These advantages make the outer rotor downhole turbine generator have high applicability and performance in special downhole environments such as high temperature and high pressure.

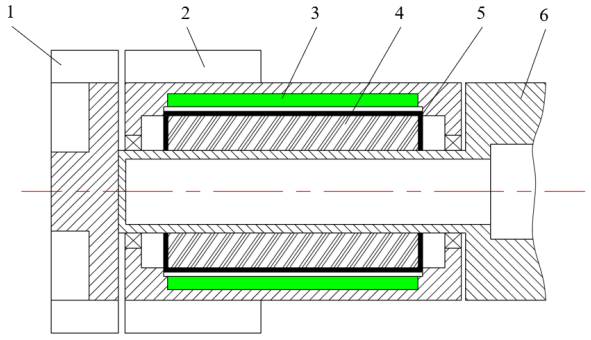

1- liquid conducting wheel ; 2-turbine ; 3-permanent magnet ; 4-Stator coil ; 5 - isolation sleeve ; 6-generator shell

Figure 1. Structure diagram of a new type of outer rotor downhole turbine generator

3. Downhole Turbine Generator Design

3.1. Rated data design of downhole turbine generator

The rated data of the downhole turbine generator is the basic parameter of the generator, which reflects the performance and capacity of the generator, and is also the goal to be achieved in the design of the generator. The rated data of the downhole turbine generator is shown in Table 1.

Table 1. Rated data of generator

Parameters	value	Parameters	value
nominal power	800W	Rated speed	2500rpm
Number of motor phases	3	Rated frequency	166.7Hz
Rated line voltage	48V	Power factor	0.9
Rated phase voltage	27.71V	Connection method	Y
Rated line current	9.62A	efficiency	0.9
Rated phase current	5.56A	Voltage adjustment rate	0.1

3.2. Turbine generator rotor design

In order to be able to play a role in magnetic concentration and have a faster dynamic response, the rotor permanent magnets are arranged in a built-in radial arrangement. Samarium cobalt is selected as the permanent magnet material, which has the advantages of high Curie temperature, large remanence, large maximum magnetic energy product and large coercivity. The parameters of the rotor are shown in Table 2.

Table 2. Main dimension parameters of rotor

Parameters	value	Parameters	value
Rotor outer diameter	10cm	Interpolar width	0.61cm
Rotor inner diameter	7.8cm	Total volume of permanent magnet	188.16cm^3
Number of magnetic poles	4	Density of permanent magnet	8.3g/cm^3
length of magnetization direction	0.6cm	Permanent magnet mass	1.56kg
Width of permanent magnet	2.45cm	Axial length of permanent magnet	16cm
interpolar gap	3.06cm	Residual magnetic flux density	1.04T
Cross-sectional area of permanent magnet	39.2cm^2	Coercivity	780KA/m
Polar arc coefficient	0.8	Relative permeability	1.06H/m

3.3. Turbine generator isolation sleeve and air gap design

Considering the working environment of the turbine generator, the material of the isolation sleeve must have good high temperature and high pressure resistance and wear resistance. At the same time, the isolation sleeve cannot affect the magnetic induction line generated by the permanent magnet generator. Finally, the material of the isolation sleeve is titanium alloy. This material has the advantages of good mechanical properties, low permeability and high temperature resistance. The thickness of the isolation sleeve is designed to be 2mm. The air gap determines the distance between the stator and the rotor, which affects the starting of the turbine generator and the cutting of the magnetic induction line. Considering the size of the permanent magnet generator and the thickness of the isolation sleeve, the air gap thickness is designed to be 2mm.

3.4. Stator design of turbine generator

Considering the convenience of coil embedding, eddy current loss and efficiency, the stator slot of the turbine generator in this design is pear-shaped slot. The slot shape is shown in Fig.2.

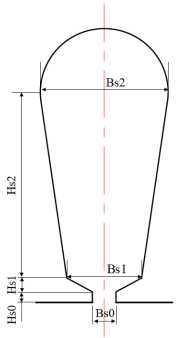

Figure 2. Stator slot type

The parameters are shown in Table 3.

Table 3. Stator slot parameters

Parameters	value	Parameters	value
Bs0	4.4mm	Hs0	1mm
Bs1	10mm	Hs1	2mm
Bs2	6mm	Hs2	10mm

The final stator design parameters are shown in Table 4.

Table 4. Main size parameters of stator

Parameters	value	Parameters	value
Stator outer diameter	7cm	Number of conductors per slot	44
Stator inner diameter	3cm	Number of parallel branches	2
Stator core length	16cm	Groove full rate	78.7%
Pitch of winding	3	Winding	1.2mm
Number of stator slots	12	winding factor	0.9
Effective area of stator slot	80.51mm^2	Number of turns	44
Stator slot spacing	1.83cm		

4. Electromagnetic Field Simulation Analysis of Turbine Generator

4.1. Turbine generator model

According to the design parameters, the generator model is established in CAD and imported into Ansoft Maxwell software. The generator model is shown in Fig.3. After defining the material, setting the boundary conditions, meshing, setting the excitation and the solver, the no-load and load analysis of the transient field of the permanent magnet generator can be carried out.

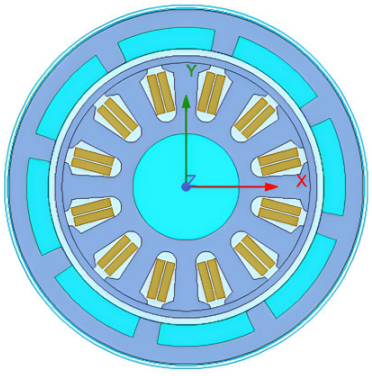

Figure 3. Two-dimensional model of generator

4.2. No-load simulation analysis

Through the simulation analysis of the no-load magnetic cloud map, magnetic field line, no-load induced electromotive force and cogging torque, it is possible to evaluate whether the electromagnetic design of the turbine generator meets the requirements. The magnetic cloud diagram of the turbine generator at rated speed obtained by no-load simulation is shown in Fig.4. It can be seen from the figure that the maximum magnetic flux density of the turbine generator is 1.9925 T, and the maximum magnetic flux density is mainly distributed in the rotor shell and near the end of the permanent magnet. In the whole region, the magnetic flux density saturation region is less, and most of the region is still in a low magnetic flux density state. In addition, the distribution of magnetic flux density along the X-axis and Y-axis shows a good uniform symmetry. This shows that the magnetic circuit design of the turbine generator is reasonable. Through the no-load simulation analysis, the distribution of the magnetic field line of the turbine generator at the rated speed is obtained, as shown in Figure 5. It can be seen from the diagram that the magnetic lines on the rotor shell and the stator teeth are relatively dense, and the magnetic lines between the air gaps pass vertically. On the whole, the closure of the magnetic field line is high, and the distribution shows good uniform symmetry. The overall leakage flux of the turbine generator is small, which indicates that the design is reasonable.

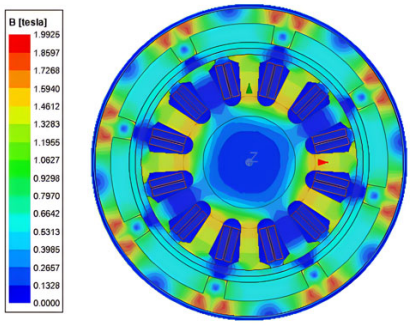

Figure 4. No-load magnetic cloud map

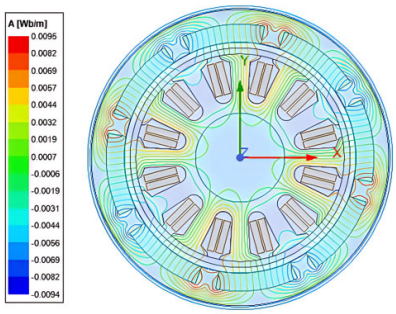

Figure 5. No-load magnetic field line diagram

The induced electromotive force waveform at the rated speed obtained by the no-load analysis is shown in Fig.6. It can be seen from the diagram that the waveform of the three-phase induced electromotive force is smooth and sinusoidal. The amplitude of the three-phase induced electromotive force is close to 39.98 V, and the effective value of the phase voltage is 28.27 V, which is higher than the designed rated phase voltage.

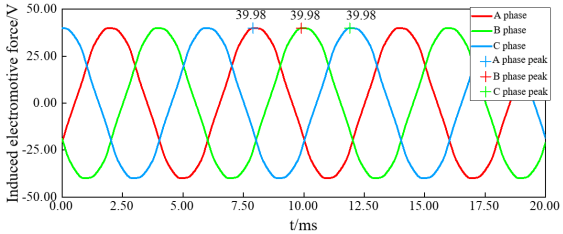

Figure 6. No-load induced electromotive force

Through the no-load simulation analysis, the cogging torque waveform at the rated speed is obtained, as shown in Fig.7. It can be seen from the diagram that in the no-load simulation, the cogging torque changes periodically near the zero axis after being stabilized, and the peak value of the cogging torque is 736.68 $\mathrm{mN \cdot m}$.

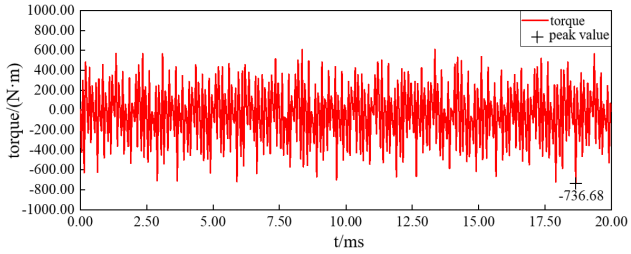

Figure 7. No-load torque waveform diagram

4.3. Load simulation analysis

When the load is running, the magnetic field generated by the armature winding interacts with the magnetic field of the permanent magnet, resulting in a change in the working state of the permanent magnet. Therefore, in addition to the additional rated external resistance, the resistance and inductance of each phase armature winding need to be considered when adding the external circuit. The resistance of each phase armature winding is determined to be 0.18Ω , the inductance is $1.91\times10^{-4}\mathrm{H}$, and the rated external resistance is determined to be 2.88Ω by the relationship between the rated power and the rated voltage. External circuits are set up in ANSYS Maxwell software, as shown in Fig.8.

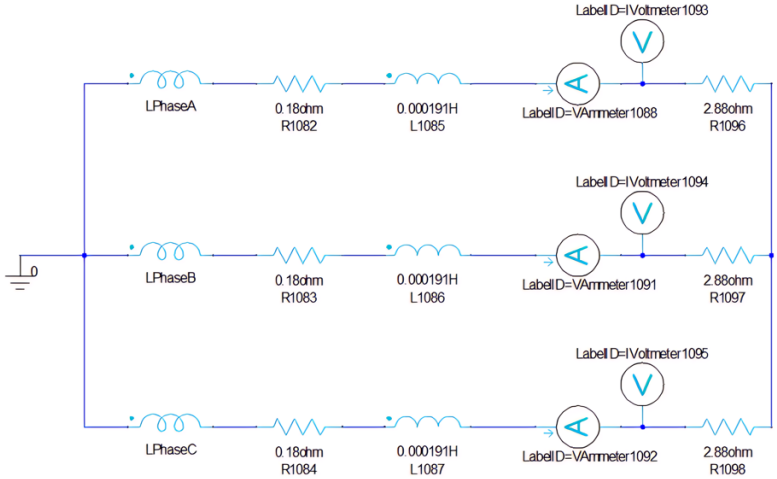

Figure 8. External load circuit diagram

The magnetic cloud diagram of the turbine generator at rated speed is obtained by load simulation, as shown in Fig.9. It can be seen from the diagram that the maximum magnetic flux density of the turbine generator is 1.9594 T, which is close to that of the no-load operation. The distribution of magnetic flux density is consistent with that of no-load operation. The maximum magnetic flux density is mainly distributed in the rotor shell and near the end of the permanent magnet. In the whole region, the magnetic flux density saturation region is less. In addition, the magnetic flux density distribution along the X-axis and Y-axis shows a good uniform symmetry, indicating that the design is reasonable. The magnetic field distribution of the turbine generator at rated speed is obtained by load simulation analysis, as shown in Fig.10. It can be seen from the diagram that the magnetic field lines are mainly distributed in the rotor shell and stator teeth, showing a dense state. The overall magnetic field line closure is high and shows good uniform symmetry, and the overall magnetic flux leakage is small, indicating that the design is reasonable.

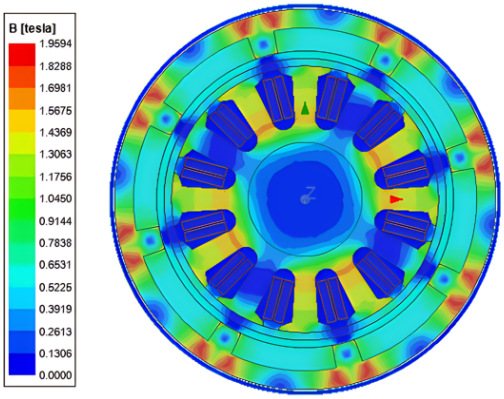

Figure 9. Load magnetic dense cloud diagram

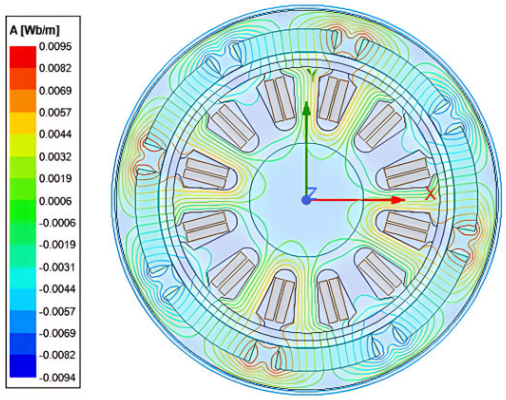

Figure 10. Load magnetic line diagram

The induced electromotive force waveform at rated speed is obtained by load analysis, as shown in Fig.11. It can be seen from the diagram that the three-phase induced electromotive force waveform is sinusoidal, smooth and relatively uniform. The amplitude of the induced electromotive force of each phase is close to 40.09 V, the effective value of the phase voltage is about 28.35 V, and the effective value of the line voltage is about 49.10 V.

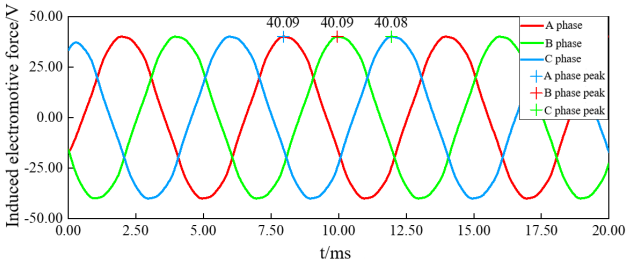

Figure 11. Load induced electromotive force

The induced electromotive force waveform at rated speed is obtained by load analysis, as shown in Fig.12. It can be seen from the diagram that the three-phase current waveform is sinusoidal, smooth and relatively uniform. The amplitude of each phase current is close to 8.97 A, the effective value of the phase current is about 6.34 A, the effective value of the line current is about 10.99 A, and the phase current is greater than the designed rated phase current value.

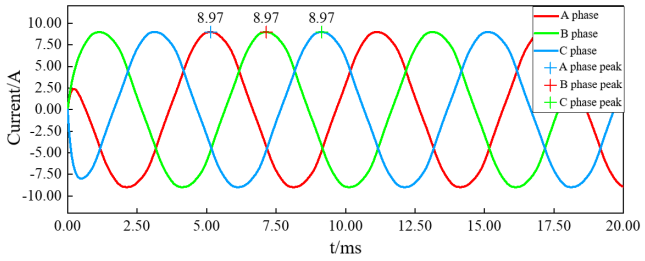

Figure 12. Load three-phase current diagram

According to the effective value of phase voltage and phase current obtained by load simulation analysis, the output power of turbine generator can be calculated, that is, the calculation formula of output power P_{out} is:

$$P_{\text{out}} = \sqrt{3} U'_N I'_N \cos\varphi \tag{1}$$

In the formula, U'_N is the effective value of the output line voltage, V; I' is the effective value of the output line voltage, A. Substituting the relevant data, the output power value is calculated to be 841.17W, which is greater than the rated power value and meets the design requirements.

The load torque waveform at rated speed is shown in Fig.13.It can be seen from the figure that when the torque reaches stability, it changes periodically, and the torque is all negative. This is because the torque of the generator hinders the rotor movement in the opposite direction, and the peak torque is 2.81 $\mathrm{N \cdot m}$.

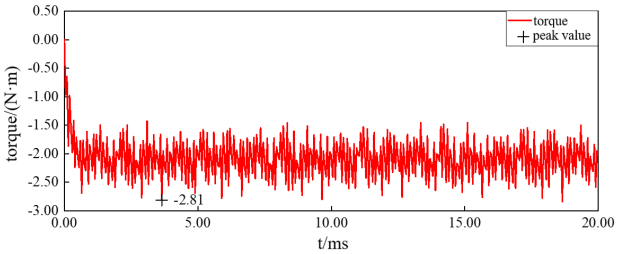

Figure 13. Load torque waveform diagram

The driving torque T of the turbine generator is equal to the sum of the no-load torque T0 and the load torque, namely:

$$T = T_0 + T_{\text{e}} \tag{2}$$

In the formula, T_0 is the no-load torque of the turbine generator, $\mathrm{N \cdot m}$; T_{e} is the load torque, $\mathrm{N \cdot m}$. With the relevant data, the turbine generator driving torque can be obtained to be 3.54 $\mathrm{N \cdot m}$.

4.4. Loss analysis

The electromagnetic analysis of the turbine generator is carried out in Ansoft Maxwell software. The copper loss obtained is shown in Fig.14. It can be seen that the peak value of copper loss in steady state is 38.96W. The obtained iron loss is shown in Fig.15.It can be seen that the peak value of iron loss in the steady state is 4.91W. After the above analysis, the total loss of the turbine generator is 43.87W after ignoring the mechanical loss and other stray losses.

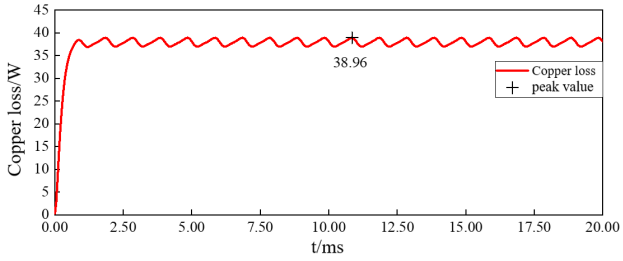

Figure 14. Copper loss diagram

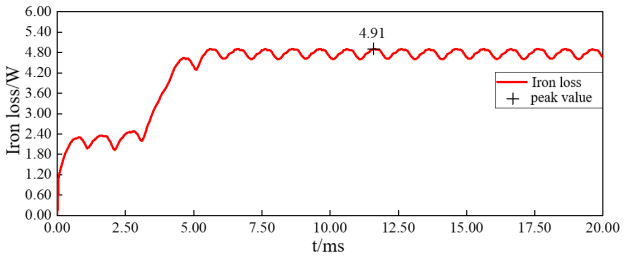

Figure 15. Iron loss diagram

The efficiency of the turbine generator is one of its important indicators. It is the ratio of the output power of the turbine generator to the sum of the output power and the total loss, that is:

$$\eta = \frac{P_{out}}{P_{out} + \sum P} \times 100\% \tag{3}$$

In the formula: η is efficiency; P_{out} is output power, W; $\sum P$ the total loss, W. The output power and total loss of the generator have been calculated before, and the efficiency is 95%. It is worth noting that the calculated efficiency here is the efficiency after ignoring the mechanical loss and other stray losses, and the real efficiency is slightly lower than the calculated efficiency.

4.5. The influence of rotational speed on the output performance of generator

The output performance of the turbine generator at different speeds is shown in Fig.16. It can be seen from the figure that as the speed increases, the output voltage amplitude, output current amplitude, efficiency, output power and driving torque all show an overall upward trend. The amplitude of the output voltage, the amplitude of the output current and the driving torque increase approximately linearly, while the growth rate of the efficiency curve gradually decreases, and the growth rate of the output power curve gradually increases. The change trend of each curve conforms to the theory, which proves the rationality of the simulation. Finally, at the rated speed of 2500rpm, the above analysis shows that it also meets the design requirements of the turbine generator.

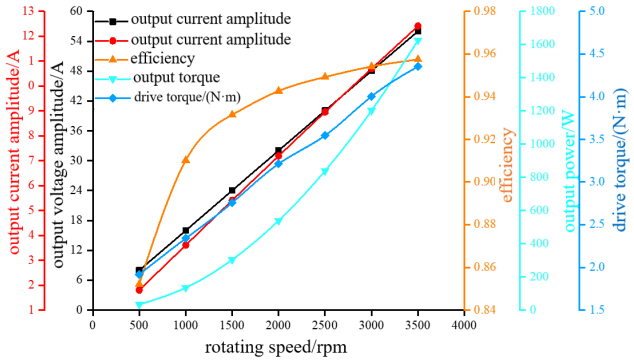

Figure 16. The output performance of the generator at different speeds

5. Conclusion

In this paper, a new type of outer rotor downhole turbine generator is designed, and the structure and parameters of the turbine generator are designed. Finally, the electromagnetic field simulation analysis of the generator is carried out by Ansoft Maxwell software, and the following conclusions are obtained:

(1) Through the analysis of no-load and load, the magnetic flux density cloud diagram and the magnetic field line diagram are obtained. Most of the magnetic flux density cloud diagram is in a low magnetic flux density state and is evenly symmetrically distributed. The magnetic field line distribution in the magnetic field line diagram also shows good uniform symmetry, and the magnetic field line closure is high, indicating that the design of the turbine generator is reasonable.

(2) Through the electromagnetic analysis of the turbine generator, the influence of the speed on the output performance is obtained. With the increase of the speed, the output voltage amplitude, the output current amplitude, the efficiency, the output power and the driving torque are all on the rise. At the rated speed of 2500rpm, the effective value of the output line voltage of the turbine generator is about 49.1V, the effective value of the line current is about 10.99A, and the output power is about 841.17W, which meets the design requirements.

Acknowledgment

Study on friction and lubrication characteristics of polycrystalline diamond rolling-sliding composite bearing under impact heavy load + 2019QHZ006

References

[1] QIAN X, ZHANG J. Exploration and Development Technology of Shale Oil and Gas in the World: Progress, Impact, and Implication[J]. IOP Conference Series: Earth and Environmental Science, 2020: 12131.

[2] ZUOQIAN W, ZIFEI F, XINGYANG Z, et al. Status, trends and enlightenment of global oil and gas development in 2021[J]. Petroleum Exploration and Development, 2022(No.5): 1210-1228.

[3] FEDOROV S, HAGSPIEL V, ROGSTAD R W H, et al. Evaluation of tieback developments for marginal oil fields with timing flexibility[J]. Energy Economics, 2024: 107344.

[4] WANG C, KE P, CAO C, et al. Study on the downhole measurement method of weight on bit with a near-bit measurement tool[J]. Geoenergy Science and Engineering, 2023: 211633.

[5] ZHANG W, REN J, ZHU F, et al. Analysis and selection of measurement indexes of MWD in rock lithology identification [J]. Measurement, 2023(No.0).

[6] CHEN W, GU Q, LI X, et al. Efficient Encoding Method for Combined Codes in the MWD Telemetry System[J]. Electronics, 2023(No.22): 4683.

[7] ZHANG L, SHEN Y, HU G, et al. The speed control research on rotary valve driven by micromotor in MWD[J]. Microsystem Technologies, 2022(No.1): 229-236.

[8] LIANG X, GHOREISHI O, XU W. Downhole Tool Design for Conditional Monitoring of Electrical Submersible Motors in Oil Field Facilities[J]. IEEE Transactions on Industry Applications, 2017(No.3): 3164-3174.

[9] SU J, WEI L, ZHANG P, et al. Multi-type defect detection and location based on non-destructive impedance spectrum measurement for underground power cables[J]. High Voltage, 2023(No.5): 977-985.

[10] NOVOBRITSKY V A, FEDOSOV D S. The main types of wind turbines-generators in the power supply system[J]. Известия высших учебных заведений: Проблемы энергетики, 2022(No.5): 71-85.

[11] WANG Z, PEI R, YUAN H, et al. Analysis and simulation of downhole vibration environment[J]. Acta Geophysica Sinica, 2023(No.1): 153-161.

[12] WEI M, CAI W, XU M, et al. Active Cooling System for Downhole Electronics in High-Temperature Environments[J]. Journal of Thermal Science and Engineering Applications, 2022(No.8): 81009.